

Finite Element Modeling of Reinforced Concrete Cladding Panels

H. Maneetes

A. M. Memari*

Department of Architectural Engineering, The Pennsylvania State University, 104 Engineering Unit A, University Park, PA, 16802, United States of America

*Email: memari@enr.psu.edu

ABSTRACT: Architectural precast concrete cladding systems are considered non-load bearing wall systems and are designed primarily to transfer their self-weight and out-of-plane lateral loads to the supporting building structure. They are typically not designed for significant structural in-plane forces resulting from cladding-structure interaction. In fact, modern earthquake-resistant design requires that these cladding panels be isolated from the lateral force-resisting system. Finite element technique was employed to study precast concrete panels and special modeling strategies were developed for panel connections to the structural frame. The precast concrete panel was designed to participate in the building lateral force-resisting. Finite element modeling techniques were adopted to better understand the strength and stiffness characteristics of these concrete cladding panels subjected to significant in-plane loading. Good correlation was obtained between finite element modeling results and existing experimental results. The analytical results were used to develop a simplified mathematical model that can be incorporated into suitable building models to evaluate its performance as a lateral force-resisting system to withstand earthquake-induced lateral loads.

Keywords: Finite Element Modeling, precast concrete cladding panels, Earthquake Resistant Design.

1 INTRODUCTION

Architectural precast concrete cladding systems are designed to transfer their self-weight and out-of-plane lateral loads (e.g., wind and earthquake) to the supporting building structure. The cladding system is often assumed to have negligible influence on the lateral stiffness of the building and hence is ignored in the structural design. However, studies (Ellis 1980, Goodno & Will 1978, Wiss & Curth 1970) have shown that these architectural components can contribute significantly to the lateral stiffness of the structure and that the panels can be subjected to significant in-plane forces. Other researchers (El-Gazairly & Goodno 1989, Meyyappa et al. 1981, Uchida et al. 1973) have shown that precast cladding panels can have significant effect on the dynamic properties of the building.

To reduce significant in-plane forces from developing in the cladding panels as a result of cladding-structure interaction, modern earthquake-resistant design requires that these cladding panels be isolated from the Lateral Force-Resisting System (LFRS). For example, PCI (PCI, 1989) recommends the use of flexible connections or connections that permit relative movements at the attachment points. These provisions are aimed at minimizing cladding-structure interaction and hence reduce the type of

cladding damage seen in past earthquakes (e.g., 1978 Miyagiken-Oki, 1987 Whittier Narrows and the 1995 Hyogoken-Nambu earthquakes, McMullin 2000).

On the other hand, rather than emphasizing the need to reduce cladding-structure interaction, some recent studies have advocated the use of cladding-structure interaction to improve overall building performance to better withstand earthquake-induced loading. For example, Goodno et al. (1992) exploited this cladding-structure interaction through the development of an advanced energy dissipating mechanism in the cladding connections. These connections are designed to maximize the benefits of cladding-structure interaction while attempting to minimize the damaging effect on the cladding panels by inertia loads. The research discussed here is also geared towards the use of cladding-structure interaction. Specifically, it is aimed at enhancing the performance of the building seismic response by using the implicit advantage of the building enclosure integrated in the lateral load resisting system of the building.

The primary objective of the research discussed was to develop an added energy-dissipating system, which can be applicable specifically to spandrel type precast concrete cladding panels, although the concept can also be applied to floor-to-floor high

panels. This spandrel type Energy-Dissipating Cladding System, or EDCS, would be able to function as a structural brace while providing some form of controlled energy dissipation. The design objective is to ensure that the cladding panel and its connections would not sustain damage as a result of the cladding-structure interaction, and to limit all irreversible inelastic deformation in the EDCS without demanding any inelastic action and ductility from the basic LFRS.

2 EDCS DESIGN

Figure 1 shows the proposed three-dimensional model of the EDCS that was developed to exploit the cladding-structure interaction while minimizing damage to the concrete panels. Connection details (e.g., tie-back, bearing connections) typical of conventional precast cladding system are employed to reduce production and installation cost. One of the support bearing connections is bolted (and welded) to the supporting beam while the other bearing connection is restrained from uplift but is detailed (through the use of slotted connection) to translate laterally to accommodate volume changes in the panel.

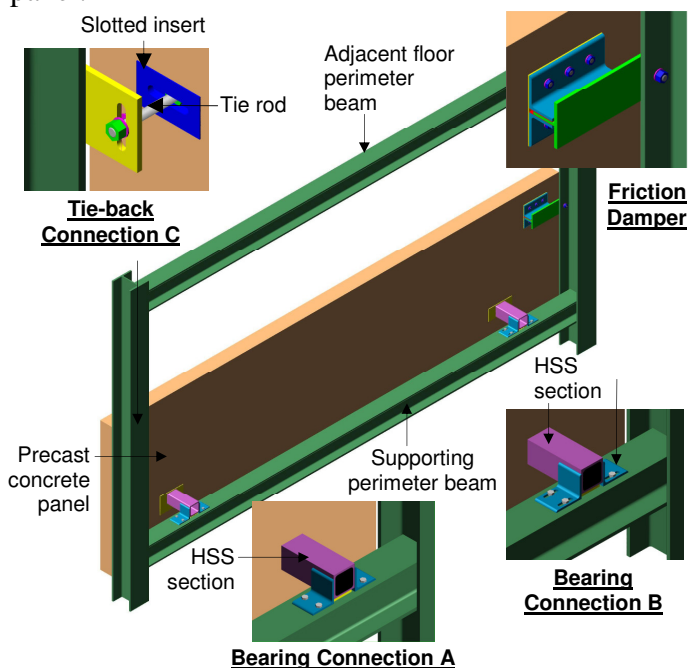


Figure 1. CAD Model of Energy Dissipating Concrete Panel (EDCS).

The precast concrete panel is designed to function as a rigid brace during low intensity earthquake motions. Under moderate or high intensity seismic motions, the in-plane forces developed in the cladding panel would exceed the design slip load of the Slotted Bolted Connection (SBC) friction damper, causing it to slip horizontally and dissipate part of the building input energy. In this regard, the friction damper has an important function of limiting the maximum load that can be transferred to the

concrete panel. The friction damper is incorporated as part of the connection between the supporting column and the cladding panel. Details on the conceptual design of the EDCS can be found in Maneetes (2007). The proposed design relies on the ability of the precast concrete panel to carry the high in-plane loads and this was investigated using finite element modeling techniques.

Precast concrete panels, in particular, architectural precast cladding panels, are not designed to take significant in-plane structural forces. This may explain why there seems to be inadequate literature on the Finite Element Analysis (FEA) or modeling of precast concrete panels. Where numerical simulation is employed, the Finite Element (FE) model of the panel is often idealized as uncracked and infinitely stiff (Petkovski & Waldron 1995, Goodno & Craig 1998). The panel connections to the structural frame appear to be the focus of most research interest since the connections are typically treated as the weakest link in the event of a catastrophic failure. The EDCS concrete panel has been specifically designed to participate in the building LFRS. An important objective of the study was to better understand the strength and stiffness characteristics of the concrete panels subjected to significant in-plane loading through FE techniques.

3 FINITE ELEMENT MODELING

Reinforced concrete structures are commonly designed to satisfy both serviceability and safety criteria. To ensure the serviceability requirement, prediction of cracking and estimation of deflection under service loads need to be considered. To meet the safety or strength requirement, an accurate estimation of the ultimate load is essential but it is also desirable to predict load-deformation characteristics of the structure.

Because of the complexities associated with the development of rational analytical procedures for reinforced concrete, many design methods still rely on the empirical approach, using the test results from a large number of experiments. Nowadays, with the availability of inexpensive and high-performance computers and well-developed FEA software, FEA is now a powerful and general analytical tool to model the behavior of structural concrete. Through FEA, important parameters like stress-strain relationships, cracking model, etc., that have significant influence on the structural concrete behavior can be conveniently and systematically investigated. However, the need for some form of experimental research still continues to provide a firm basis for design equations. Experimental data also supply the much needed information, e.g., material property, to validate the mathematical

models for FEA. On the other hand, reliable FE models can considerably cut down the number of experiments required, hence reducing both time and cost of solving a given problem.

Several recent studies (Wolanski 2004, Fanning & Kelly 2000, Idelsohn et al. 1998) have focused on a commercial FE package, ANSYS, for modeling reinforced concrete beams and prestressed beams. These studies have reported good correlations between the analytical results and experimental data. This is largely attributed to the availability of a rather sophisticated element, known as SOLID65, from ANSYS built-in element library. This element was developed primarily to model the complex nonlinear behavior of brittle materials, especially plain concrete and reinforced concrete. In particular, the complex cracking phenomenon of concrete can be modeled with its built-in cracking models. The availability of this exclusive concrete element, together with good correlations reported by these studies, has made ANSYS Version 9 (2005) a suitable FE software for modeling precast concrete cladding panels for the present research.

3.1 FE Model for Precast Concrete Panel

The spandrel panel studied is shown in Figure 2, with a height of 2.13 m (7 ft). The panel height takes into account the depth of supporting beam, concrete floor slab, raised-floor requirement (in typical office) and finishes, and also height to openings (i.e., window). The panel is 7.32 m (24 ft) long and 203.2 mm (8 in.) thick with the length corresponding to that of a typical building bay. Structural welded wire reinforcement is commonly used to control shrinkage and cracking due to ease of placement (PCI 2004) and hence is specified. Supplementary reinforcements were also added to better confine the concrete at the highly stressed connection anchoring points and prevent the development of localized cracking. Different schemes of placing the extra reinforcing bars to effectively transfer the in-plane applied force through the panel were investigated in the study. Square Hollow Steel Section (HSS) was specified for all bearing connections while 25.4 mm (1 in.) diameter threaded rod was used for the tie-back rod. Two configurations to anchor the bearing connections to the concrete panel were studied. In the first case, the hollow section was embedded directly into the concrete while the second approach utilized headed studs as anchoring system to reduce stress concentration through better distribution of the anchoring forces into the concrete matrix.

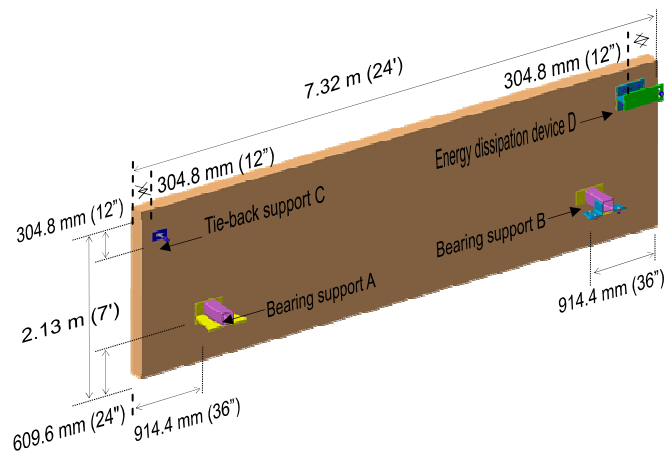


Figure 2. Dimensions of Spandrel Precast Concrete Panel.

The FE models for the precast concrete panel are shown in Figure 3. The types of finite elements used to model different components of the panel are summarized in Table 1 and explained in detail in this section. A total of 6,003 ANSYS SOLID65 elements were used to model a single panel. Each SOLID65 cube element measured 51 mm (2 in.) although 25 mm (1 in.) cube was specified for the concrete cover. The Hognestad stress-strain relationship with multi-linear kinematic hardening rule was used. The built-in failure criteria for SOLID65 were represented by the William-Warnke five-parameter models. The material properties used to define the constitutive models are summarized in Figure 4 for a concrete strength of 34.48 MPa (5,000 psi) and these are estimated based on ACI 318 (2002). Fanning (2001) reported that the concrete properties estimated from prevailing design codes were appropriate for defining the analytical model. The cracking model in the SOLID65 element was utilized whereas the crushing model was deactivated to improve numerical stability. For modeling the reinforcing steel, the following three different approaches could be used: the discrete model; the embedded model; and the distributed or smeared model. The discrete model with one dimensional reinforcement elements (bar or beam elements) was most widely used by other researchers (Wolanski 2004, Tavarez 2001) and hence was adopted in the present study. The rebar elements were superimposed in the concrete model. The rebar and the concrete mesh shared the same nodes and concrete occupied the same regions occupied by the rebar. ANSYS LINK8 three-dimensional uniaxial tension-compression element was used to model all discrete reinforcing bars in the concrete and placed in accordance to the layout specified for each analysis case. A concrete cover of 25.4 mm (1 in.) was used. A bilinear kinematic strain hardening model ($f_s = 414$ MPa (60 ksi); $E_s = 200$ GPa (29,000 ksi); tangent modulus $E_s' = 20$

MPa (2.9 ksi); $\nu = 0.3$) was used to present the Grade 60 steel bars.

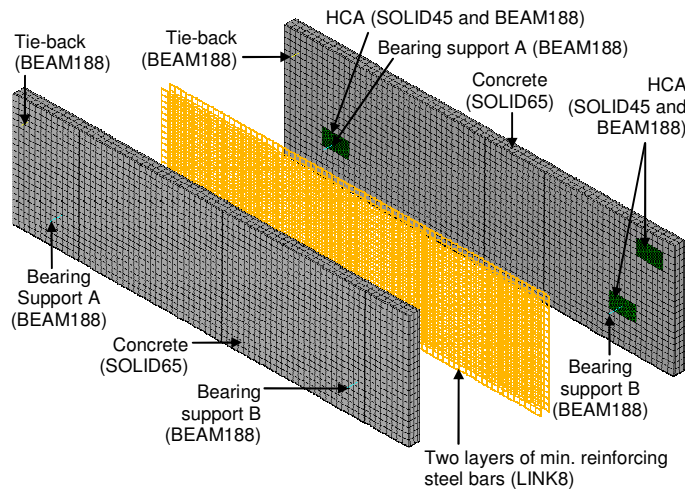


Figure 3. FE Models of the EDCS.

Table 1: ANSYS Finite Elements Used

Components	ANSYS element type
Concrete panel	SOLID86
Reinforcing steel bar	LINK8
Bearing support, tie-back	BEAM188
HCA anchor plate	SOLID45
HCA headed stud	BEAM188

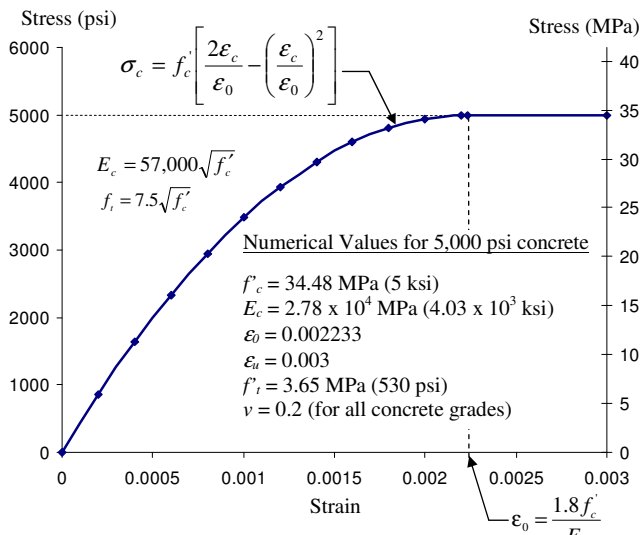


Figure 4. Concrete Stress-strain Model Used for the Cladding Panel.

A concentrated load and moment were applied to the surface of the anchorage plate simultaneously. The moment accounted for the out-of-plane load eccentricity of 254 mm (10 in.) For the bearing supports, the free end of the BEAM188 element was specified as pinned or fixed for support A, depending on the analysis case, and roller

(horizontal direction) condition for support B. The tie-back was specified as capable of resisting out-of-plane force only.

3.2 Comparison of FE Model Results with Existing Test Results

Prior to the FEA of the precast concrete panels and modeling of connection and other components, a separate study was carried out to evaluate the appropriateness of the modeling strategy for the reinforced concrete. The FEA studies (using ANSYS) of Wolanski (2004), Fanning & Kelly (2000), and Idelsohn et al. (1998) focused primarily on conventional reinforced concrete beams, which are structurally different from the thin precast concrete panels. The behavior of reinforced concrete deep beam, with similar depth-to-width (or thickness) ratio to precast concrete panel, appeared to be a more suitable choice. Accordingly, the simply-supported deep beam of Leonhardt & Walther (1966) that was discussed by Reineck et al. (2002) was modeled in this study. The reinforced concrete deep beam modeled is a 1.6 m (5.25 ft) wide by 1.6 m (5.25 ft) deep by 100 mm (3.9 in.) thick as shown in Figure 5.

This deep beam was supported on 160 mm (6.3 in.) long bearing plates with a center-to-center clear span of 1.44 m (4.72 ft). The beam was loaded on the top with a uniform load applied over the clear span distance of 1.28 m (4.20 ft). The main (bottom) flexure reinforcement consist of four 8 mm (0.32 in.) diameter reinforcing bars having a yield stress of 427.5 MPa (62 ksi). The vertical faces of the deep beam were reinforced with 5 mm (0.2 in.) diameter reinforcing bars at 259 mm (10.2 in.) in both directions. The reported (Leonhardt and Walther 1966) concrete strength at the time of testing was 30.2 MPa (4,380 psi). The deep beam was reported to fail at a total load of 1,170 kN (263 kips).

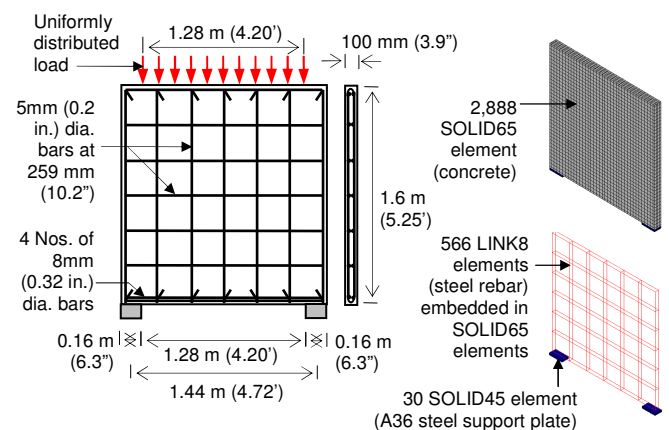


Figure 5. Reinforced Concrete Deep Beam and ANSYS FE Model.

The analytical load-deflection curve shown in Figure 6 matches reasonably well with the experimental data up to 890 kN (200 kips), beyond which the analytical model exhibited a stiffer response than the actual test beam. The difference between the numerical and experimental failure load is less than 0.4%. Figure 7 shows the resulting crack formation, at the failure load, which appeared to correlate well with the test result. The study on the deep beam indicated that the proposed modeling strategies for reinforced concrete were appropriate.

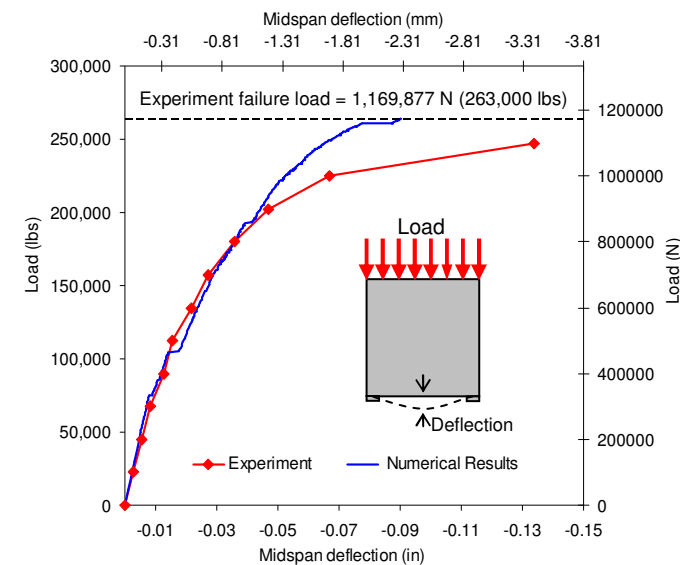


Figure 6. Comparison of Experimental and Analytical Load Deflection Relationship.

3.3 FE Models for Connections

The HSS bearing supports were modeled with ANSYS BEAM188 elements and bilinear kinematic strain hardening model ($f_s = 414$ MPa (60 ksi); $E_s = 200$ GPa (29,000 ksi); tangent modulus $E_s' = 20$ MPa (2.9 ksi); $\nu = 0.3$). Where A36 anchorage plate was used (e.g., for HCA), ANSYS SOLID45 elements with bilinear kinematic strain hardening model ($f_s = 248$ MPa (36 ksi); $E_s = 200$ GPa (29,000 ksi); tangent modulus $E_s' = 20$ MPa (2.9 ksi); $\nu = 0.3$) were used and the BEAM188 elements were embedded directly into the SOLID45 elements. This was required to prevent unnecessary rotation at the plate-beam interface. It should be pointed out that the “stick” BEAM188 element had practically zero “foot-print” that led to unrealistically high stress concentration occurring in the adjacent SOLID45 plate elements and excessive flexure of the plate. In reality, the (welded) base of the actual HSS covered a finite area of the plate and this portion of the plate could be considered as infinitely stiff; any significant plate bending would occur outside this area. Thus, it would not be unreasonable to specify a high rigidity for the SOLID45 plate elements

confined within this area. The threaded-rod for the tie-back connection was modeled with BEAM188 element.

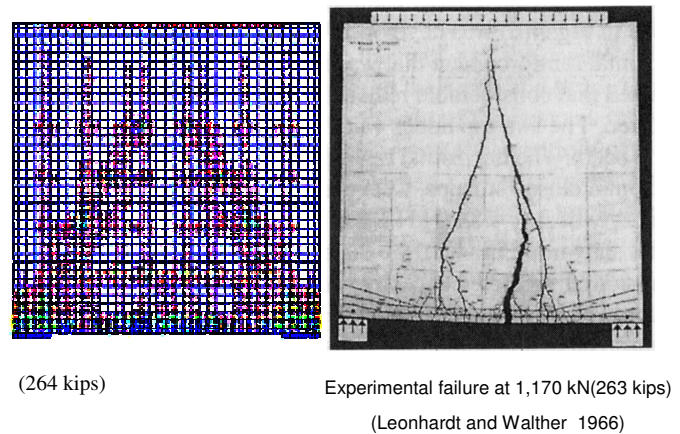


Figure 7. Analytical Crack Development in FE model of a Deep Beam and Comparison with test results

3.4 FE Models for Headed Concrete Anchor System

Headed Concrete Anchors (HCA) or studs were employed in the design of the EDCS as an effective concrete anchorage system to distribute the high in-plane loads and reactions from the bearing connections to the surrounding concrete matrix. The HCA design comprised of a 508 mm (20 in.) long by 305 mm (12 in.) wide by 51 mm (2 in.) thick A36 anchorage plate with eight equally-spaced 22 mm (7/8 in.) diameter by 152 mm (6 in.) headed studs. Based on PCI design guidelines (PCI, 2004), the nominal design tensile and shear capacities of the HCA group were calculated as 282 kN (63.4 kips) and 94.3 kN (21.2 kips) for corner condition, respectively. Additional steel rebars with adequate development length were attached to plates in two orthogonal directions to increase the shear capacity in excess of 267 kN (60 kips). Different amount and arrangement of additional reinforcing steel were investigated in the study.

The HCA was modeled as part of the FEA of the precast concrete panel. Due to lack of literature on modeling HCA using ANSYS during the time of the study, another numerical study was performed to add confidence to the suitability of the FE modeling technique adopted for the HCA. Three different locations of the HCA were investigated. These locations correspond to three distinct loading conditions or failure modes, namely front-edge loading, corner-edge loading and side-edge loading. The loading condition is defined by the ratio of the side-edge distance to the back-edge distance. The unreinforced concrete panel (Figure 8) measured 2.13 m (7 ft) and 4.26 m (14 ft) for side-edge loading condition by 2.44 m (8 ft) by 203 mm (8 in.) thick with a concrete strength of 34.5 MPa (5,000

psi). The right edge of the panel was restrained from translations and rotation in all directions.

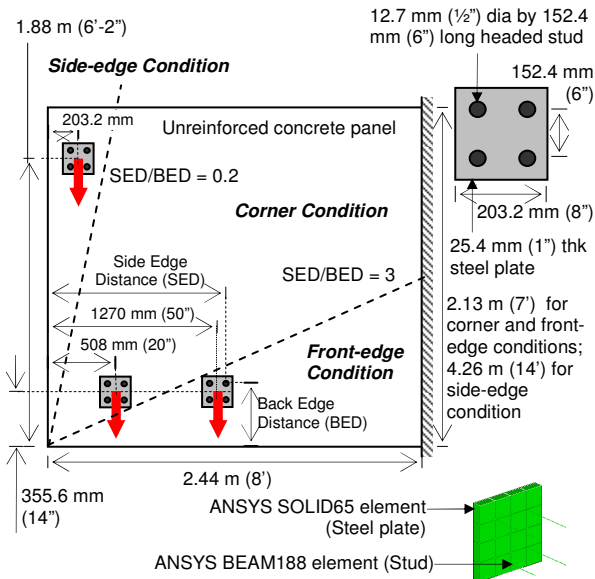


Figure 8. FE Model for HCA Groups.

The HCA consisted of four Type B 13 mm (1/2 in.) diameter by 152 mm (6 in.) long headed studs welded to a 152 mm (6 in.) by 203 mm (8 in.) and 25 mm (1 in.) thick A36 steel plate. The studs were modeled with ANSYS BEAM188 elements and bilinear kinematic strain hardening model ($f_s = 352$ MPa or 51 ksi; $E_s = 200$ GPa or 29,000 ksi; tangent modulus $E_s' = 20$ MPa or 2.9 ksi; $\nu = 0.3$). The constitutive model for the unreinforced concrete panel and A36 steel plates were identical as the precast concrete panel described earlier (except that no steel rebar was modeled). The shear load application on the HCA was specified as concentric. The nominal design values were estimated from PCI design handbook (PCI, 2004) for the three different loading conditions and are summarized in Table 2.

Table 2: Nominal Design Values of HCA Groups.

Loading condition	Side Edge Distance (SED), mm (in.)	Back Edge Distance (BED), mm (in.)	SED/BED ratio*	Nominal design values**, kN (kips)
Front-edge	1320 (52)	406 (16)	3.250	102.7 (23.1)
Corner	558.8 (22)	406 (16)	1.375	86.7 (19.5)
Side-edge	254 (10)	1930 (76)	0.130	167.2 (37.6)

* For SED/BED < 0.2, side-edge loading condition generally controls; 0.2 < SED/BED < 3, a corner condition exists. Front-edge condition with SED/BED > 3 (PCI 2004).

** Based on concrete failure (steel failure at 231.3 kN or 52 kips for all cases)

Table 3 summarizes the analytical crack patterns at the maximum load at which the FEA terminated. These maximum loads are not the failure loads due to non-convergence of solution. However, these maximum values are close to the nominal design values. More importantly, the predictions show the correct order of strength with the side-edge loading case having the highest resistance. Each analytical model exhibited three unique crack patterns corresponding to the three different loading conditions. The numerical results indicated that the simple FE modeling strategy adopted for the HCA would be appropriate for the cladding panel.

Table 3: FE Results of HCA.

Loading condition	Numerical crack pattern at max. load	
Front-edge		
	Max. FEA load	Design value (Table 2)
	115.2 kN (25.9 kips)	102.7 kN (23.1 kips)
Corner		
	Max. FEA load	Design value (Table 2)
	94.7 kN (21.3 kips)	86.7 kN (19.5 kips)
Side-edge		
	Max. FEA load	Design value (Table 2)
	173.0 kN (38.9 kips)	167.2 kN (37.6 kips)

3.5 Friction Damper

The nonlinear behavior of the friction damper is generally well-understood and could be modeled using ANSYS COMBI165 spring-damper element. Adding the friction damper in the FE model would effectively limit the maximum load of the EDSCS to the damper slip load. In this case, the EDSCS

components (i.e., concrete panel and connections) would merely respond elastically as designed. Although not critical for the EDCS design, it would be more useful to obtain information about the inelastic response of these components, for example the onset of inelastic response. Thus, the friction damper was excluded from the FE model to achieve higher loads and inelastic component response.

4 NUMERICAL RESULTS

4.1 Parametric Study on Reinforcing Layout and Connection Details

A total of eight FE models (cp1 to cp8) corresponding to different reinforcing layout and connection details were initially analyzed. The initial tangent stiffness, elastic-limit load (i.e., load at the onset of nonlinear response) and maximum load for each case are summarized in Table 4 whereas Figure 9 shows a typical analytical load deflection curve. The numerical results showed that the amount of cracking at the connections controlled the maximum load at which each analysis could reach.

cp1 was modeled to represent conventional architectural precast cladding panel. It was specified with minimum (welded wire mesh) reinforcement with no additional steel reinforcing bars near the connections. The FEA for cp1 terminated at a very low load (9.2 kips) due to extensive cracking around the loading point. Although this load may not necessarily be the ultimate lateral load capacity of the panel, the stiffness of the panel was deteriorating rapidly beyond this load level. This was not desirable since the concrete panel was expected to behave essentially elastic up to about 40 kips. The numerical crack pattern observed was consistent with a corner failure.

For model cp2, diagonal bars (or sections) were added to provide a direct load path between the pinned supports with the aim of improving the lateral load carrying capacity. The analytical results show that the increase in lateral stiffness was insignificant. The stress in the diagonals revealed that diagonal bars or struts would only be effective if the bars were debonded from the concrete. With the bars bonded to the concrete mass, the bar force would be completely transferred to the concrete mass along the developed length of the diagonal bar. The developed length for #7 Grade 60 bars and 34.5 MPa (5,000 psi) concrete is only 1.22 m (4 ft), compared to the panel length of 7.32 m (24 ft). In cp3, additional reinforcing steel bars were added to the loaded connections, and the FE model was able to reach higher load prior to termination of the analysis due to a lesser extent of cracking. The elastic-limit load had increased by more than two

times though it only improved the initial stiffness by 20%. It was found that embedding the HSS into the concrete resulted in high stress concentration and early reduction in lateral stiffness as observed in cases cp1 to cp3.

Table 4: Initial Tangent Stiffness, Elastic-limit Load and Maximum Load.

Model Label	Initial tangent stiffness		Elastic-limit load		Maximum load	
	kN/mm	kips/in.	kN	kips	kN	kips
cp1	43	243	20.9	4.7	40.5	9.2
cp2	45	257	20.9	4.7	44.9	10.1
cp3	51	292	46.7	10.5	104.5	23.5
cp4	40	226	82.3	18.5	130.8	29.5
cp5	489	2,792	177.9	40.0	275.5	61.9
cp6	191	1,089	180.1	40.5	266.0	59.8
cp7	41	233	87.2	19.6	126.3	28.4
cp8	191	1,088	180.1	40.5	303.4	68.2

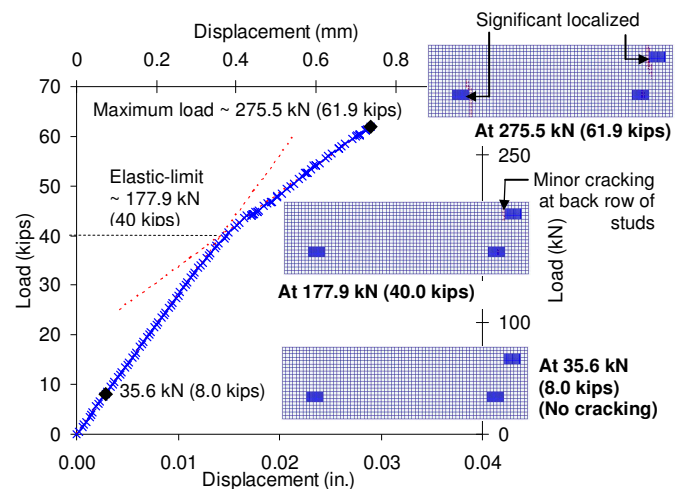


Figure 9. Load-deformation Curve for FE Model cp5.

The introduction of the HCA in cp4, to better distribute the anchoring force, significantly increased the elastic-limit load by as much as 76% (compared to cp3). A slight reduction (23%) in overall stiffness was not expected since the HSS exhibited higher flexural stiffness than the headed stud anchor. Changing the support condition of the cantilevered bearing supports from pinned (cp4) to fixed (cp6) led to the significant (more than five times) increase in the lateral stiffness. Such an increase is not unreasonable since the stiffness of a fixed-fixed beam bending in double-curvature is at least four times that of a cantilever beam bending in

simple curvature. Removing the (right) cantilevered bearing support, in cp5, resulted in a two times increase in stiffness, compared to cp6. An additional mid-layer of reinforcing bars was added in cp7 and cp8 with the intention of confining the concrete around the loaded points. Comparing cp5 and cp6 with cp7 and cp8, respectively, the results indicated no advantage of adding an additional mid-layer of reinforcing bars and the conventional two layers, one on each face, seems adequate. For cp8, at 40 kips (i.e., twice the designed slip load), only minor cracks formed in the surface concrete elements adjacent to the loaded HCA as shown in Figure 10. The depth of these cracks was confined to the thickness of the concrete cover and did not lead to observable stiffness or strength degradation. Thus the reinforcement and connection details specified in cp8 would allow the EDCS (except for the friction damper) to behave elastically as required and could be adopted as a feasible solution.

4.2 Stress Distributions and Displacement Contours

The stress distributions within the concrete panels were investigated to evaluate whether the elastic beam theory could be used to describe the stresses in the panel. The result of the analysis (Maneetes 2007) showed that, consistent with Saint-Venant's principle, there exists an undisturbed Beam or B-region away from the supports where the elastic stress distributions are nearly linear and can be predicted by elastic beam theory.

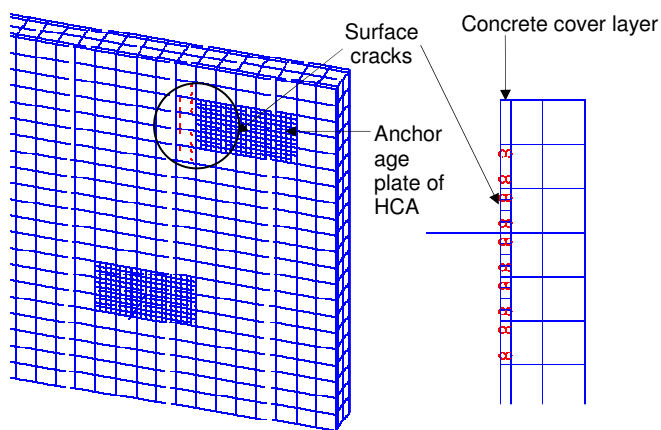


Figure 10. Analytical Concrete Cracking for Model cp8.

The Disturbed or D-regions extended about eight times the thickness of the panel away from the loaded points; the assumption that the D-region covered a distance equal to the overall height of the panel, H , would be conservative. Comparison of the stress distribution at selected cross-sections in the B-regions (Maneetes 2007) predicted by elastic beam theory with that based on the FEA results, showed that the theory appears to correlate rather well with

the numerical results for the distribution in the B-region. In the D-regions between the supports, the normal stress distribution from the FEA generally followed the linear profiles described by the elastic theory, except for small localized regions near the HCA. This in turn suggests that the in-plane load-deformation of the concrete panel could also be approximated by the elastic beam theory. This knowledge facilitated the development of analytical expressions to estimate the stiffness of the panel.

Figure 11 shows the displacement contours of cp8 in the global x-, y- and z-directions at 177.9 kN (40 kips). The observed twisting effect of the panel was due to the eccentric loading and the flexibility of the bearing supports. The largest deflection of 2 mm (0.08 in.) was observed in the z-direction at the top edge of the panel.

The stress trajectory plots of the principal stresses for model cp8 are presented in Figure 12. The arrows indicate the general direction of the vector in the principal direction 1. Moving away from the loaded connections, the stress trajectories became uniform and predominately uniaxial, again suggesting the presence of an undisturbed or B-region. On the other hand, the trajectories in the vicinity (within a distance of eight times the panel thickness) of the connections were highly directional. For short spandrel panel (with length less than two times the height) or panels with openings, the principal stress plots would provide valuable information about the load path within the panel.

Figure 13 shows the maximum and minimum principal stress contours of the panel at 40 kips. The contours show that the panel between the connections is predominately under uniaxial tension. The plots also show the extent of stress concentration around each connection.

4.3 Estimating Stiffness of EDCS Components

The FEA results supported the EDCS concept to function as a structural brace capable of withstanding the significant in-plane forces. The performance of the EDCS as a passive seismic protection system must be evaluated at the building level. Despite the fact that it is possible to model the EDCS and a representative building or structure using FEA techniques discussed earlier, it would be more logical (and efficient) to first reduce the FE model of the EDCS to a simpler mathematical formulation. The strategy adopted was to represent the in-plane behavior of the EDCS as a two dimensional assemblage of truss and spring elements

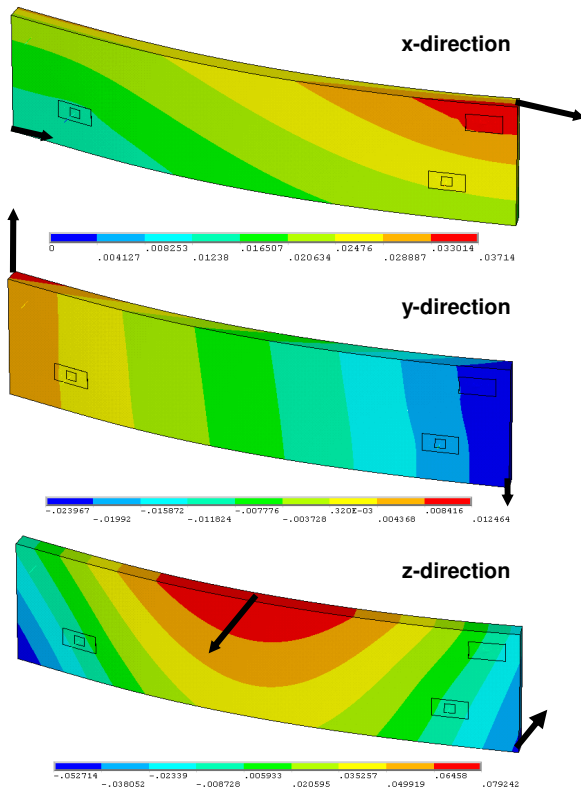


Figure 11. Displacement Contours for Model cp8.

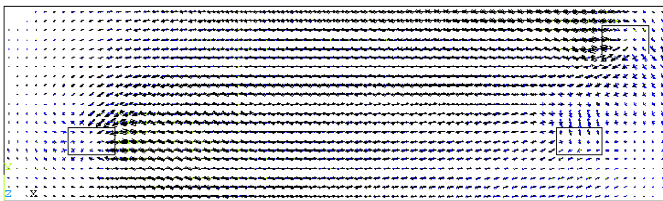


Figure 12. Vector Plot of Principal Stresses.

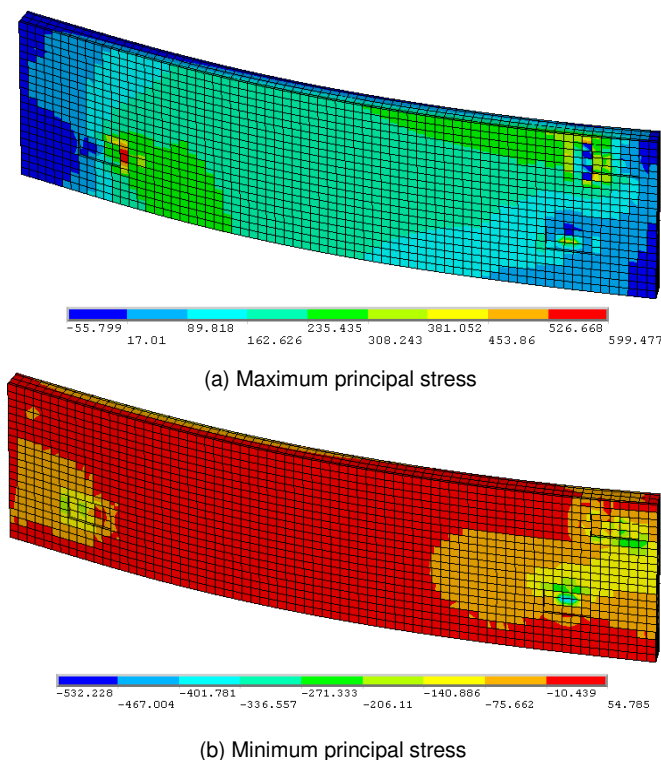


Figure 13. Contours of Maximum and Minimum Principal Stresses.

as shown in Figure 14. The (infinitely) rigid truss elements only serve to transmit the axial forces developed in the EDCS to the supporting beam and column. The axial deformations in these elements were made negligible and were oriented as shown to correctly replicate the direction of the forces at the connections. The entire load-deformation characteristic of the EDCS is presented here by a single elastic perfectly-plastic spring element with stiffness K_{EDCS} . The overall lateral stiffness (K_{EDCS}) of EDCS can be considered as comprising of a series of springs, each capturing the load-deformation of a major component of the system.

As illustrated in Figure 15, the major components contributing to the lateral stiffness of the assembly are the reinforced concrete panel ($K_{concrete}$), the bearing support ($K_{bearing}$), the headed stud assemblies (K_{stud}), and the damper assembly (K_{damper}). Although the ultimate failure load of each major component of the EDCS could be found (from prevailing design codes), it was not necessary to construct the entire load-deformation curve since the lateral load in the EDCS was capped at the design slip load of friction damper as illustrated. All other components were designed to respond elastically throughout the operating range of the damper. The load-deformation of the friction damper is well documented in literature and can be approximated by a perfectly-plastic function as shown in Figure 15.

To determine the influence of the various parameters on the stiffness of the EDCS, a total of thirteen additional FE models were created in ANSYS. These models were similar to cp5 with respect to reinforcement layout and connection details except for the panel length (varies between 2.7 m (9 ft) to 7.3 m (24 ft)), height (2.1 m (7 ft) to 4.0 m (13 ft)), thickness (154 mm (6 in.) to 254 mm (10 in.)), concrete compressive strength (27.6 MPa (4 ksi) to 41.1 MPa (6 ksi)) and relative position of the connections. These parameters were varied for each model so that it gave a slightly different lateral stiffness value. Details of the initial tangent stiffness, elastic-limit load and maximum load from the analysis for this series of models are discussed by Maneetes (2007). The initial tangent stiffness (also the lateral stiffness) for the thirteen models varies between 309 kN/mm (1,762 kips/in.) and 572 kN/mm (3,269 kips/in.). As mentioned earlier, the elastic beam theory was found to be appropriate for the cladding panel, and together with the numerical results, analytical expressions to estimate the stiffnesses of the various EDCS components were developed. The study has also revealed that the assumption of an uncracked and infinitely stiff (Petkovski & Waldron 1995, Goodno & Craig 1998) precast concrete panel may not be appropriate. The concrete panel studied was found to contribute to as

much as 58% of the overall flexibility of the EDCS. The flexible anchorage (i.e. HCA) was found to reduce the lateral stiffness of the precast concrete panel by more than 80%. Applications of the developed simplified model for building modeling can be found in (Maneetes 2007).

5 SUMMARY AND CONCLUDING REMARKS

The following concluding remarks can be drawn from the numerical study:

1. For analysis of a deep beam, the SOLID65 element with its explicit cracking model is suitable.
2. Good correlations between the FEA results and existing experimental results for the deep beam suggest that the concrete properties estimated from existing design guidelines are appropriate for the FE model.
3. The analytical models for the deep beam tend to exhibit a significantly stiffer response than the test beam.
4. Embedding the HSS into the concrete resulted in high stress concentration and early reduction in lateral stiffness. The HCA would provide better distribution of anchoring force than embedded HSS section and significantly increased the elastic-limit load by as much as 76%.
5. The simple finite element modeling strategy adopted for the HCA was found to be adequate.
6. Diagonal bars or brace placed between the support and the load application would only be effective if the bars were debonded from the concrete. With the bars bonded to the concrete mass, the bar force would be completely transferred to the concrete mass along the developed length of bar as the spandrel panel is long. The nonlinear FEA showed that with adequate reinforcement and proper detailing of the connections, the precast concrete panels can be designed to remain essentially elastic up to the specified slip load of the friction damper.
7. Changing the cantilevered bearing supports from pinned to fixed led to as much as five times increase in the lateral stiffness of the panel.
8. Additional center layer of reinforcing bars in the precast concrete panel is not necessary. The conventional two curtains of reinforcement, one on each face, is adequate.

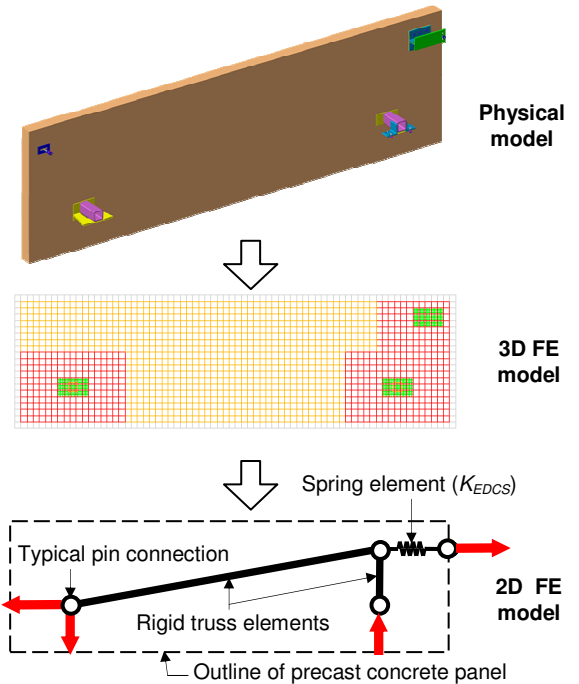


Figure 14. Simplifying the Mathematical Model of EDCS.

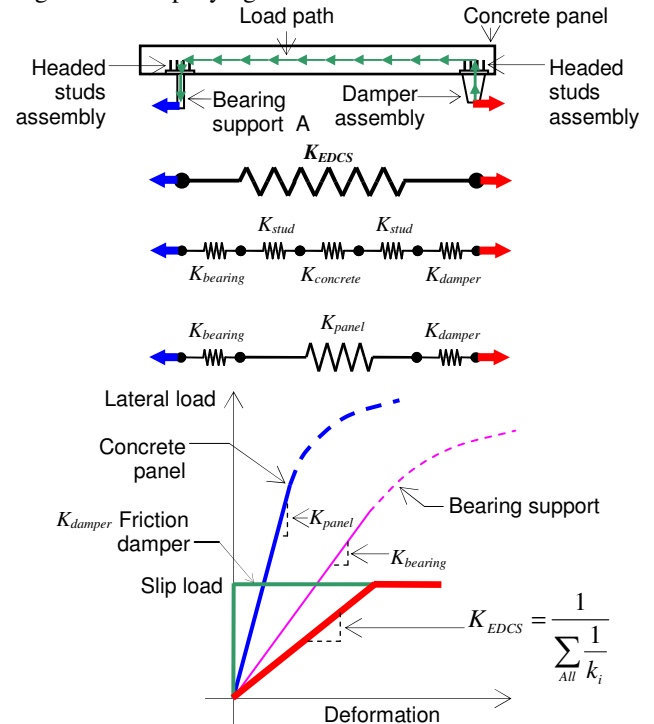


Figure 15. Components of EDCS Stiffness.

9. To accurately describe the stress and stiffness characteristics of the panel, combination of elastic beam theory and stress field based theory should be used.
10. Closed-form expressions were found to correlate well with the FEA results in the region between the lateral supports. Thus, the spandrel panel could be approximated by simple elastic beam theory alone to obtain the in-plane load-deformation characteristics.

11. By taking into account the flexibility of the HCA, the overall lateral stiffness of the panel could be significantly reduced by more than 80%. Therefore the stiffness, in addition to the strength, of the concrete anchorage system must be considered in the design for the EDCS.
12. The precast concrete panel with HCA can contribute as much as 58% to the overall lateral flexibility of the EDCS unit. This suggest that to assume an infinitely stiff precast concrete panel may not be appropriate.

REFERENCES

- [1] American Concrete Institute (ACI) Committee 318. (2002), Building Code Requirements for Structural Concrete (ACI 318-02) and Commentary (ACI 318R-02), ACI, Farmington Hills, Michigan.
- [2] ANSYS. (2005), ANSYS Manual Version 9.0, ANSYS Inc., Canonsburg, PA.
- [3] El-Gazairly, L.F., and Goodno, B.J. (1989), "Dynamic Analysis of a High-rise Building Damaged in the Mexico Earthquake Including Cladding-Structure Interaction," Proceedings, International Symposium on Architectural Precast Concrete Cladding – Its Contribution to Lateral Resistance of Buildings, Nov 8-9, PCI, Chicago, IL, pp. 257-286.
- [4] Ellis, B.R. (1980), "An Assessment of the Accuracy of Predicting the Fundamental Natural Frequencies of Buildings and the Implications Concerning the Dynamic Analysis of the Structures," Proceedings, Institution of Civil Engineers, Part II, 69, pp. 763-776.
- [5] Fanning, P., and Kelly, O. (2000), "Smearred Crack Models of RC Beams with Externally Bonded CFRP Plates," Computational Mechanics, 26, pp. 325-332.
- [6] Fanning, P. (2001), "Nonlinear Models of Reinforced and Post-tensioned Concrete Beams," Electronic Journal of Structural Engineering, 2, pp. 111-119.
- [7] Goodno, B.J. and Will, K.M. (1978), "Dynamic Analysis of High-rise Building including Cladding-Structure Interaction Effects," Proceedings of the conference on Computers in Civil Engineering, June 26-29, 1978, Atlanta, GA, pp. 623-638.
- [8] Goodno, B.J., Craig, J.I., El-Gazairly, L.F., and Hsu, C.C. (1992), "Use of Advanced Cladding Systems for Passive Control of Building Response in Earthquakes," Proceedings, 10th World Conference on Earthquake Engineering, July 19-24, Madrid, Spain, pp. 4195-4200.
- [9] Goodno, B.J., Craig, J.I. (1998), Ductile Cladding Connection Systems for Seismic Design, Report No. NIST GCR 98-758, National Institute of Standards and Technology, Gaithersburg, MD.
- [10] Idelsohn, S.R., Onate, E., and Dvorkin, E.N., eds. (1998), Computational Mechanics. New Trends and Applications, International Center for Numerical Methods in Engineering, Barcelona, Spain.
- [11] Leonhardt, F., and Walther, R. (1966), "Wandartiger Träger," Bulletin No. 178, Deutscher Ausschuss für Stahlbeton, Wilhelm Ernst & Sohn, Berlin, Germany.
- [12] Maneetes, H. (2007), Development of a Seismic Dissipating Mechanism for Precast Concrete Cladding Panels, Ph.D. Thesis, The Pennsylvania State University, University Park, PA.
- [13] McMullin, (2000), <http://www.engr.jsu.edu/mcmullin/research/cladding/>.
- [14] Meyappa, M., Palsson, H., and Craig, J.I. (1981), "Modal Parameter Estimation for a Highrise Building Using Ambient Response Data Taken During Construction," Proceedings, 2nd Specialty Conference on Dynamic Response of Structures: Experimentation, Observation, Prediction, and Control, January 15-16, Atlanta, GA, pp. 141-151.
- [15] Petkovski, M., and Waldron, P. (1995), "Seismic Behavior of Reinforced Concrete Frames with Energy Dissipating Cladding," European Seismic Design Practice, Balkema, Rotterdam, Netherlands.
- [16] Precast/Prestressed Concrete Institute (PCI). (1989), Architectural Precast Concrete, 2nd ed., PCI, Chicago, IL.
- [17] Precast/Prestressed Concrete Institute (PCI). (2004), PCI Design Handbook: Precast and Prestressed Concrete, 6th ed., PCI, Chicago, IL.
- [18] Reineck, K.H., (Ed.) (2002), Examples for the Design of Structural Concrete with Strut-and-tie Models, American Concrete Institute, Farmington Hills, MI.
- [19] Tavarez, F.A. (2001), Simulation of Behavior of Composite Grid Reinforced Concrete Beams Using Explicit Finite Element Methods, Master of Science Thesis, University of Wisconsin-Madison, Madison, WI.
- [20] Uchida, N., Aoygai, T., Kawamura, M., and Nakagawa, K. (1973), "Vibration Test of Steel Frame Having Precast Concrete Panels," Proceedings, 5th World Conference on Earthquake Engineering, June 25-29, Rome, Italy, pp. 1167-1176.
- [21] Wiss, J.F., and Curth, O.E. (1970), "Wind Deflections of Tall Concrete Frame Buildings," Journal Structural Division, ASCE, 96(ST7), pp. 1461-1480.
- [22] Wolanski, A.J. (2004), Flexural Behavior of Reinforced and Prestressed Concrete Beams Using Finite Element Analysis, Master of Science Thesis, Marquette University, Milwaukee, WI.